

# Estimation of electrodynamic exciter parameters by means of circle-fit method

Martin Pustka<sup>1</sup>, Martin Černík<sup>1</sup>, Norbert Palsovics<sup>1</sup>

<sup>1</sup> Measurement Department, VÚTS, a.s., Svárovská 619, 460 01 Liberec, Czech Republic

## ABSTRACT

The electrodynamic inertial exciter is an electromechanical transducer extensively implemented in a number of technical applications. The exciter commonly operates in a wide frequency range and its performance strongly depends on the input excitation parameters and output loading. The identification of basic transducer parameters is thus necessary for the design and development of electromechanical devices or for modelling and simulation of exciter frequency response using a lumped-element model. The paper introduces an experimental and calculation method for electrodynamic exciter parameters estimation based on the circle-fit of measured frequency response functions, an approach common in a classic experimental modal analysis. The method is suitable for simple electromechanical or electroacoustic systems whose natural frequency falls within the operational frequency range. The procedure was verified on displacement to current and voltage to current transfer functions measured on a commercial electrodynamic exciter.

**Section:** RESEARCH PAPER

**Keywords:** Electrodynamic exciter; transfer function; curve fitting; parameter estimation

**Citation:** M. Pustka, M. Černík, N. Palsovics, Estimation of electrodynamic exciter parameters by means of circle-fit method, Acta IMEKO, vol. 14 (2025) no. 1, pp. 1-6. DOI: [10.21014/actaimeko.v14i1.1847](https://doi.org/10.21014/actaimeko.v14i1.1847)

**Section Editor:** Laura Fabbiano, Politecnico di Bari, Italy

**Received** March 26, 2024; **In final form** December 10, 2024; **Published** March 2025

**Copyright:** This is an open-access article distributed under the terms of the Creative Commons Attribution 3.0 License, which permits unrestricted use, distribution, and reproduction in any medium, provided the original author and source are credited.

**Corresponding author:** Martin Pustka, e-mail: [martin.pustka@vuts.cz](mailto:martin.pustka@vuts.cz)

## 1. INTRODUCTION

The electrodynamic exciter (body shaker, tactile transducer) is an electromechanical transducer that converts an electric audio signal to mechanical vibration and acoustic waves. This transducer is based on the same principle as an electrodynamic loudspeaker without a diaphragm and is composed of an oscillating inertia mass, a voice coil, and a suspension system. To generate an audible sound, the electrodynamic exciter is attached to a flexible panel. The inertia force of the oscillating mass is then transmitted to the panel, resulting in the excitation of bending waves and sound emission. The electrodynamic inertial exciters are used in many technical applications including acoustic wave generation [1], measurement of the point mechanical impedance of mechanical structures [2], mobility control and active noise suppression [3], modal and vibration testing [4] or sensor calibration [5].

The energy conversion between the mechanical and electrical parts of the transducer is reversible. The dynamic exciter can therefore operate reciprocally, and the input and output quantities are related by the electromagnetic coupling coefficient (a transducer constant). However, the inertial mass with the suspension spring forms a damped vibration system, whose

natural frequency usually falls within the operational frequency range. This behaviour influences the electrical and electromechanical frequency response of the transducer near its mechanical resonance.

For the application in either sensing or actuating mode, it is necessary to estimate the transfer characteristics of the transducer. These determine the frequency dependence of electrical and mechanical system parameters, necessary for design purposes. The transfer functions are further used in modelling and simulation of dynamic structures by means of two-port network models [6]. The transfer functions can be obtained by calculation using lumped-element models [7], where the circuit parameters are assessed most often experimentally [2], or by fitting the measured frequency response functions [8] using appropriate methods.

In this article, the circle-fit method, a procedure common for classic experimental modal analysis [9], is applied to obtain model transfer functions, modal parameters (resonant frequency and damping ratio), and circuit parameters from measured frequency response functions in the vicinity of the mechanical resonance. The topic presented in the paper is a part of the research work in the field of vibroacoustic structures with haptic feedback,

where the electrodynamic exciter is coupled to the vibrating composite panel. The optimization of the dynamic response of the whole structure in the lower frequency range (up to 250 Hz) is of the most importance for the final design of the resonant system.

In Section 2 a dynamic model of the electrodynamic exciter and transfer function derivation are presented. The curve fitting method and the procedure of parameter estimation are introduced in Section 3. In the next section, the proposed procedure is applied to the data obtained by measurement of a tactile transducer. Section 5 summarizes the results of this work and draws conclusions.

## 2. FREQUENCY TRANSFER FUNCTIONS OF AN ELECTRODYNAMIC EXCITER

The schematic representation of an electrodynamic inertial exciter in the form of a linear lumped-element model is given in Figure 1. A single-degree-of-freedom mechanical oscillator is coupled to an electrical circuit by means of an electromagnetic field. This dynamic system can be represented as a linear two-port network, which relates the mechanical quantities (force  $F$  and velocity  $v = \dot{x}$ ) to the electrical quantities (voltage  $u$  and current  $i$ ). Assuming that all these quantities are harmonic functions of time  $e^{j\omega t}$ , the governing equations can be expressed in a matrix form [7] as

$$\begin{bmatrix} F \\ v \end{bmatrix} = \begin{bmatrix} 1 & Z_m \\ 0 & 1 \end{bmatrix} \begin{bmatrix} 0 & k_a \\ k_a^{-1} & 1 \end{bmatrix} \begin{bmatrix} 1 & Z_e \\ 0 & 1 \end{bmatrix} \begin{bmatrix} u \\ i \end{bmatrix}, \quad (1)$$

where

$$Z_m = j\omega m + b + \frac{k}{j\omega} \quad (2)$$

is the mechanical impedance, where  $m$  is the oscillating mass,  $b$  is the viscous damping, and  $k$  is the stiffness of the suspension spring,

$$Z_e = R_0 + j\omega L_0 \quad (3)$$

is the electrical impedance of the voice coil, where  $R_0$  is the loss resistance, and  $L_0$  is the inductance, and

$$k_a = B l \quad (4)$$

is the transducer constant, where  $B$  is the flux density and  $l$  is the active length of coil current wire. The symbol  $\omega$  stands for the angular frequency and  $j$  for the imaginary unit.

The mechanical part of the exciter (mass  $m$ , viscous damping  $b$  and spring stiffness  $k$ ) forms a single degree of freedom system with an undamped resonant frequency  $\omega_r$  and viscous damping ratio  $\xi$  given by

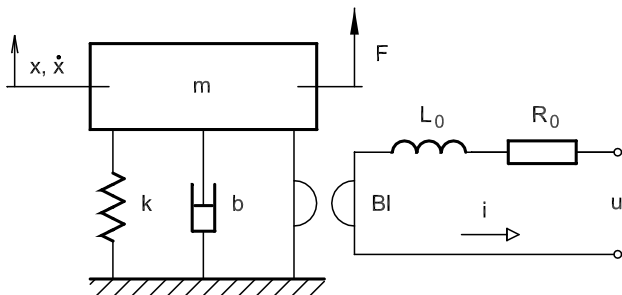


Figure 1. Linear electromechanical model of electrodynamic exciter.

$$\omega_r = \sqrt{\frac{k}{m}} \text{ and } \xi = \frac{b}{2m\omega_r}. \quad (5)$$

In actuating mode, the exciter output is related to the input current amplitude and frequency. The frequency dependence of both mechanical and electrical quantities is then commonly expressed in proportion to the input current. In our case, we need to find the frequency dependence (the transfer function) of displacement  $x$  and voltage  $u$  on the input current  $i$ . For mechanically free transducer ( $F = 0$ ) we can derive from Equation (1) by using Equations (2) to (4) a displacement to current transfer function (assuming  $v = j\omega x$ )

$$H(\omega) = \frac{x}{i} = \frac{B l}{-\omega^2 m + j\omega b + k} \quad (6)$$

and a voltage-to-current transfer function (i.e. impedance)

$$Z(\omega) = \frac{u}{i} = R_0 + j\omega L_0 + j\omega \frac{(B l)^2}{-\omega^2 m + j\omega b + k}. \quad (7)$$

The fraction terms in Equations (6) and (7) represent a "modal contribution" to the overall response at a given angular frequency  $\omega$ . The impedance frequency spectrum is therefore a sum of the electrical impedance  $Z_e$  and the modal part.

An example of measured transfer functions  $H$  and  $Z$  in the vicinity of transducer mechanical resonance is shown in Figure 2 and Figure 3. The diagrams are plotted against frequency  $f$ , taking  $\omega = 2\pi f$ . The experimental data were obtained on

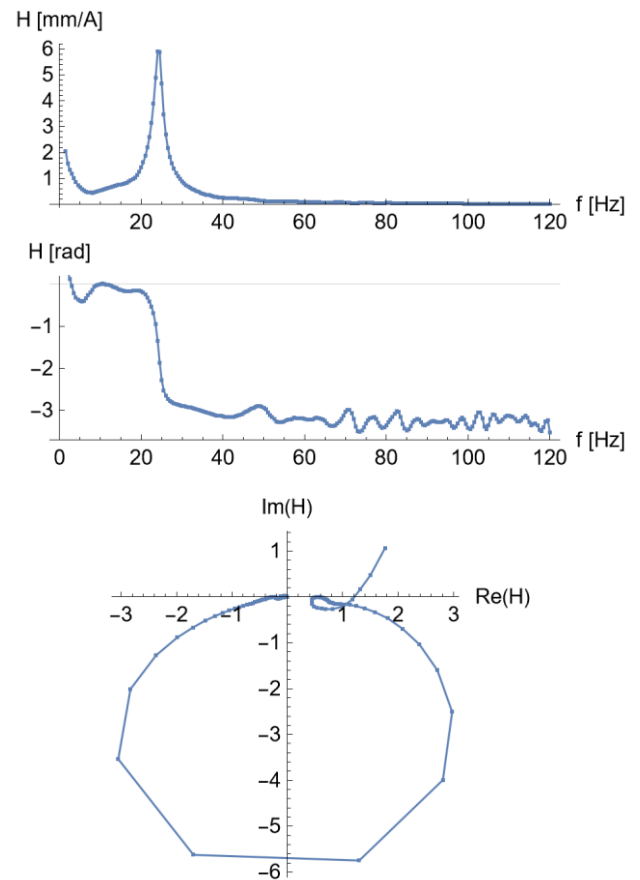


Figure 2. Measured displacement to current transfer function  $H$ , Dayton Audio BST-1 exciter, top - amplitude and phase frequency plot, bottom - Nyquist plot.

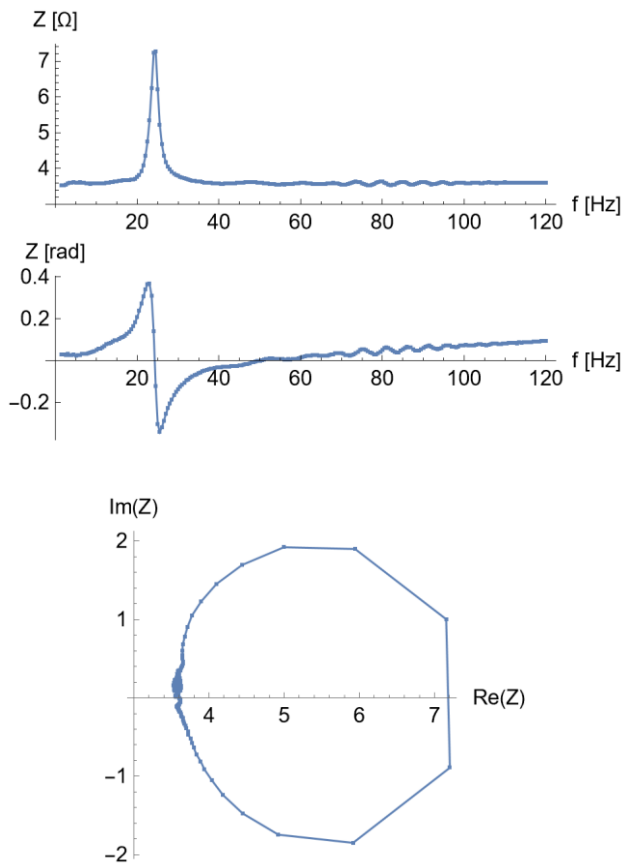


Figure 3. Measured voltage to current transfer function (impedance)  $Z$ , Dayton Audio BST-1 exciter, top - amplitude and phase frequency plot, bottom - Nyquist plot.

Dayton Audio BST-1 exciter [10] under measurement conditions mentioned below. The transfer functions are depicted as amplitude and phase frequency plots (Bode plot with linear scale) and as alternative representation in the complex plane (Nyquist plot).

### 3. CURVE FITTING OF EXPERIMENTAL DATA

The unknown quantity values in Equations (6) and (7) (mass  $m$ , damping  $b$ , stiffness  $k$ , transducer constant  $B l$  and electrical elements  $R_0$ ,  $L_0$ ) are commonly assessed experimentally (by measurement of electrical circuit parameters at transducer terminals and by identification of mechanical oscillator parameters) or from the data in the manufacturer's datasheet.

Alternatively, mainly in the case of manufacturer data unavailability, the parameter values can be estimated by fitting the measured response curves in a selected frequency range. The fitting process is based on approximation of measured transfer functions by means of the least squares method using the appropriate procedure. A large number of advanced fitting methods are available [11], in our case, it is sufficient to make use of a basic circle-fit method. This procedure takes advantage of the fact that in the vicinity of resonance, the transfer function has approximately a circular shape (a “modal circle”) in the Nyquist plot. The orientation of the circle in the complex plane is along an imaginary axis (transfer function  $H$  in Figure 2) or real axis (transfer function  $Z$  in Figure 3). We use this feature hereinafter for comparison with the theoretical shape of mechanical receptance (displacement to force transfer function)

and mobility (velocity to force transfer function) in the complex plane.

The fitting process consists of the following steps [9]: An appropriate number of measured points in the vicinity of the resonant frequency  $\omega_r$  is selected and displayed in the complex plane. A circle is found that fits the measured points and circle parameters (diameter  $R_C$ , center coordinates  $x_C$ ,  $y_C$ ) are obtained. Then, the estimates of the resonant frequency  $\omega_r$  and viscous damping ratio  $\xi$  are calculated from the circle-fit. The resonant frequency  $\omega_r$  corresponds to the point with the highest rate of spacing between measured data points in Nyquist plot (see red points in Figure 4), the damping ratio  $\xi$  is proportional to angles between specific data points. Finally, the residual terms are calculated from the circle diameter and center coordinates.

In fact, the transfer functions  $H$  and  $Z$  introduce the viscous damping model with damping ratio  $\xi$ , while the circle-fit uses the hysteretic damping model with damping loss factor  $\eta = 2 \xi \frac{\omega}{\omega_r}$ . At resonance, both damping models are equivalent and  $\eta = 2 \xi$ . For viscous damping, the mobility has an exact circular shape, while the receptance is only approximate. For hysteretic damping, this behaviour is exactly the opposite. However, for small values of viscous damping ratio in the order of percent (a value typical for most dynamic exciters) the difference between the two damping models can be neglected. We can also neglect the difference between undamped  $\omega_r$  and damped natural frequency  $\omega_n = \omega_r \sqrt{1 - \xi^2}$ .

The displacement to current transfer function  $H(\omega)$  has the same behavior as mechanical receptance, where the circle in the Nyquist plot is oriented along the negative imaginary axis. The circle-fit function has the receptance form [9]

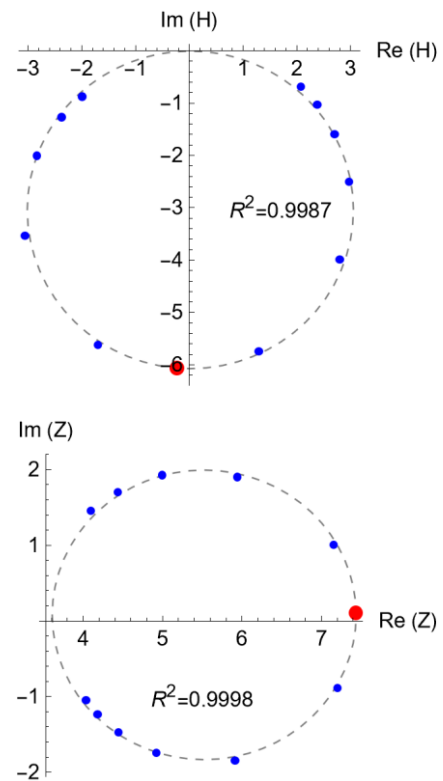


Figure 4. Circle-fit of transfer functions in the Nyquist plane, blue - measured data points, grey dashed - fitting circle, red - resonant frequency pinpoint.

Table 1. Calculation parameters of circle-fit.

Function	$f_r$ in Hz	$\xi$	$R_C$	$x_C$	$y_C$	$R^2$
Fit $H$	24.25	0.039	3.0341 mm/A	0.0189 mm/A	-3.0393 mm/A	0.9987
Fit $Z$	24.25	0.038	1.9144 $\Omega$	5.5232 $\Omega$	0.0803 $\Omega$	0.9998

$$H(\omega) = \frac{H_0}{1 - \left(\frac{\omega}{\omega_r}\right)^2 + 2j\xi} \quad (8)$$

where  $H_0 = 4 R_C \xi$  is a residuum and  $\xi = \eta/2$ . The behaviour of impedance transfer function  $Z(\omega)$  is similar to the mechanical mobility. The circle in the Nyquist plot is oriented along the positive real axis and the circle origin is displaced from the coordinate origin due to the presence of the voice coil impedance  $Z_e$ . The circle-fit function can be obtained by derivation of Equation (8) and by including the terms corresponding to the impedance  $Z_e$ , see Equation (7). We then arrive at

$$Z(\omega) = Z_2 + j\left(\frac{\omega}{\omega_r}\right)Z_1 + j\left(\frac{\omega}{\omega_r}\right)\frac{Z_0}{1 - \left(\frac{\omega}{\omega_r}\right)^2 + 2j\xi} \quad (9)$$

where  $Z_0 = 4 R_C \xi$ ,  $Z_1 = y_C$  and  $Z_2 = x_C - R_C$ .

The fit functions are proportional to the natural frequency  $\omega_r$  (5), which relates mass  $m$  with spring stiffness  $k$ . When the value of either mass  $m$  or stiffness  $k$  is available, the remaining quantity values can be calculated from the circle-fit functions. The comparison of the displacement to current transfer functions (6) and (8) leads to

$$b = \frac{2\xi k}{\omega_r} \text{ and } Bl = H_0 k, \quad (10)$$

comparing Equation (7) with (9) we get

$$b = \frac{2\xi k}{\omega_r}, Bl = \sqrt{\frac{Z_0 k}{\omega_r}}, L_0 = \frac{Z_1}{\omega_r} \text{ and } R_0 = Z_2. \quad (11)$$

In most cases, the inertial mass  $m$  is determined by weighing and the spring stiffness  $k$  is then calculated from Equation (5).

#### 4. APPLICATION EXAMPLE

The theoretical assumptions stated above were verified on experimental data obtained by measurement of electrodynamic exciter Dayton Audio BST-1 [10] transfer functions. The exciter used for the study was slightly modified compared to the original design. The application of softer support springs reduced the resonant frequency. To be able to measure the inertial mass displacement by means of the optical sensor, a hole was drilled in the bottom cover which influenced the mechanical damping due to lowering of air resistance.

The exciter frame was fixed to a heavy base, the inertial mass could oscillate freely without external loading. The exciter was driven by a swept sine voltage signal in the range of 0 to 500 Hz with a sweep rate of 250 Hz/s, which was generated by a signal generator and amplified by a class D mono amplifier with TPA3116 circuit. The excitation voltage at the transducer terminals was approximately 2 Vrms.

The axial displacement of the inertial mass was sensed by the laser displacement sensor Micro-Epsilon ILD2220-10. The input voltage was sampled directly at the terminals and the current was

measured across the shunt resistor IsabelleHüte 0.02  $\Omega$  using the four-wire method. The data acquisition was carried out using DEWE-2600 measurement analyser.

The time records were processed by means of frequency analysis and frequency auto- and cross-spectra of displacement, voltage, and current were calculated. As the single spectrum corresponds to one period of the excitation signal, no time window was applied. The final transfer functions were determined as a frequency spectra ratio using  $H_1$  estimate function [12]. The transfer functions  $H$  and  $Z$  obtained by measurement are shown in Figure 2 and Figure 3 in the frequency range to 120 Hz, the frequency resolution is 0.5 Hz.

The data measured in the vicinity of resonant frequency (11 data points, corresponding to the frequency band of 5 Hz) were used for circle-fitting and estimation of resonant frequency and damping ratio. The data evaluation was performed in Wolfram Mathematica using LinearModelFit function [13]. The results of the fitting process are given in Figure 4 and Table 1.

The quality of data regression by circle-fit is high, as indicated by the coefficient of determination  $R^2$  close to one. The resonant frequency estimates are the same for both transfer functions and equal to 24.25 Hz, see also red points in Figure 4. The calculation procedure allows the natural frequency to be estimated with a precision of approx. 10 % of data frequency resolution [9]. The estimated viscous damping ratios are also very close, the value of  $\xi$  being ca. 0.04. The fits of measured transfer functions with models given by Equations (8) and (9) are shown in Figure 5 and Figure 6. The approximation of measured characteristics with model fit functions is very good in the given frequency range.

In addition to resonant frequency and damping ratio, it is further possible to calculate other quantity values from Equations (10) and (11) using circle-fit parameters. To verify the results, an additional measurement of exciter frequency-impedance characteristics was performed using HIOKI-3522-20 LCR HiTester. The exciter mounting was the same as for previous tests and the measurement was carried out at a low current level (tens of mA). The impedance values were sampled

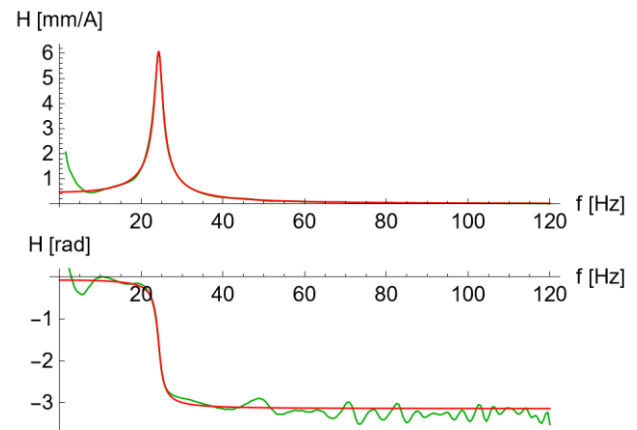


Figure 5. Fit of displacement to current transfer function  $H$ , Dayton Audio BST-1 exciter, green - measurement, red - model function given by Eq. (8).

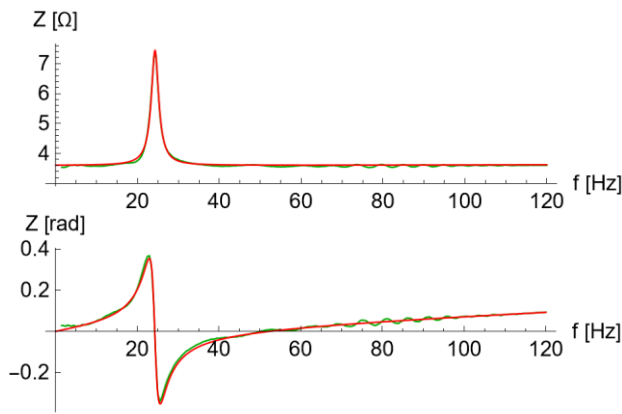


Figure 6. Fit of voltage to current transfer function  $Z$ , Dayton Audio BST-1 exciter, green - measurement, red - model function given by Eq. (9).

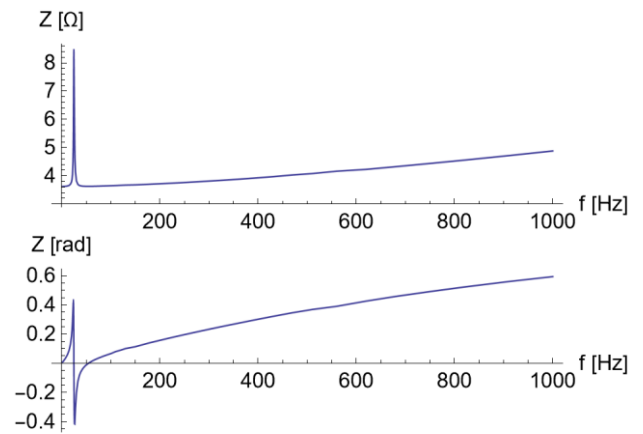


Figure 7. Frequency-impedance characteristics, Dayton Audio BST-1 exciter.

Table 2. Comparison of exciter parameters.

Source	$f_r$ in Hz	$\xi$	$m$ in kg	$b$ in $N s m^{-1}$	$k$ in $N m^{-1}$	$B l$ in T m	$R_0$ in $\Omega$	$L_0$ in mH
Fit $H$	24.25	0.039	0.366	4.37	8 500	4.05	-	-
Fit $Z$	24.25	0.038	0.366	4.27	8 498	4.05	3.61	0.527
Impedance analyser	24.7	0.038	-	-	-	4.13	3.64	0.466

sequentially at a constant input frequency. The application of constant frequency is different from dynamic excitation using a swept sine signal and for nonlinear transducers, it can lead to different results. The measured impedance characteristics is given in Figure 7, compared to Figure 3.

From the measured impedance characteristics in Figure 7, following parameters can be determined: The resonant frequency estimate  $f_r$  corresponds to the frequency of impedance maximum. The mechanical quality factor  $Q_m = \frac{1}{2\xi}$  can be calculated from the peak-magnitude frequency  $f_r$  divided by 3dB-bandwidth. The loss resistance  $R_0$  corresponds to transducer resistance at very low frequency, inductance  $L_0$  can be obtained as reactance maximum above resonance divided by its angular frequency. The relation for transducer constant deduced from Equation (7) has a form

$$B l = \sqrt{\left| (Z_{in} - Z_e) \frac{\omega_r m}{Q_m} \right|}, \quad (12)$$

where  $Z_{in}$  is transducer electrical impedance at resonant frequency and  $Z_e$  is the electrical impedance of the voice coil at resonant frequency given by Equation (3). The comparison of exciter parameters obtained from circle-fit using Equations (10) and (11) with values obtained from impedance measurement is given in Table 2. The inertial mass  $m$  was determined by weighing.

The resulting exciter parameters are in a good agreement and the difference is acceptable for design purposes. The biggest difference is observed between inductance values  $L_0$  (a relative deviation of approx. 12 %), in this case it is probably caused by a different type of excitation signal (fast harmonic sweep vs. stepped harmonic excitation). In general, the performance of Dayton exciter proved to be linear and repeatable.

## 5. CONCLUSIONS

The experimental and calculation method for electrodynamic exciter parameters estimation, based on the circle-fit of the measured frequency response function, was introduced in the paper. This approach is suitable for simple electromechanical or electroacoustic systems whose natural frequency falls within the operational frequency range and can be applied to various types of transfer functions.

The procedure was verified on displacement to current and voltage to current transfer functions measured on Dayton Audio BST-1 electrodynamic exciter. The calculated parameters were in good agreement with the data obtained by impedance measurement and the difference was acceptable for device development.

The method proved to be an effective and fast tool in practical applications, particularly in combination with appropriate excitation signals such as swept sine, stepped sine or pseudorandom. The accuracy of parameter estimation, however, is dependent on the linearity of electrodynamic exciter. The nonlinear performance and excitation level dependence can significantly influence the measured frequency response functions and thereby the parameter estimates.

## ACKNOWLEDGEMENT

This work was supported by the Czech Ministry of Industry and Trade in the framework of the institutional support for long-term conceptual development of research organization - recipient VÚTS, a.s.

## REFERENCES

- [1] M. R. Bai, T. Huang, Development of panel loudspeaker system: Design, evaluation and enhancement, J. Acoust. Soc. Am. 109 (2001) 6, pp. 2751-2761. DOI: [10.1121/1.1371544](https://doi.org/10.1121/1.1371544)

- [2] R. Boulandet, M. Michau, P. Herzog, P. Mischeau, A. Berry, A sensorless method for measuring the point mobility of mechanical structures, *J. Sound Vib.* 378 (2016), pp. 14-27. DOI: [10.1016/j.jsv.2016.05.034](https://doi.org/10.1016/j.jsv.2016.05.034)
- [3] R. Boulandet, M. Michau, P. Mischeau, A. Berry, Active reduction of sound transmission in aircraft cabins: a smarter use of vibration exciters, *INTER-NOISE and NOISE-CON Congress and Conference Proceedings* 249 (2014) 4, ISBN 978-0-909882-02-0, pp. 3751-3759.
- [4] G. F. Lang, D. Snyder, Understanding the physics of electrodynamic shaker performance, *Sound and Vibration* 35 (2001) 10, ISSN 1541-0161, pp. 24-33.
- [5] G. P. Ripper, R. S. Dias, G. A. Garcia, G. A. Primary accelerometer calibration problems due to vibration exciters, *Measurement* 42 (2009) 9, pp. 1363-1369. DOI: [10.1016/j.measurement.2009.05.002](https://doi.org/10.1016/j.measurement.2009.05.002)
- [6] J. Martino, K. Harri, Two-port modeling and simulation of an electrodynamic shaker for virtual shaker testing applications, *J. Sound Vib.* 460 (2019), p. 114835. DOI: [10.1016/j.jsv.2019.07.001](https://doi.org/10.1016/j.jsv.2019.07.001)
- [7] J. Merhaut, *Theory of Electroacoustics*, McGraw-Hill, New York, 1981, ISBN 978-0070414785.
- [8] J. Martino, K. Harri, The shaker parameters estimation, a first step to virtual testing, *MATEC Web of Conferences* 148 (2018), p. 05003. DOI: [10.1051/mateconf/201814805003](https://doi.org/10.1051/mateconf/201814805003)
- [9] D. J. Ewins, *Modal Testing: Theory, Practice and Application*, Research Studies Press, Baldock, 2000, ISBN 978-0-863-80218-8.
- [10] Dayton Audio, BST-1 High Power Pro Tactile Bass Shaker 50 Watts, 2023. Online [Accessed 16 March 2024] <https://www.daytonaudio.com/product/1245/bst-1-high-power-pro-tactile-bass-shaker-50-watts>
- [11] A. K. Zrayka, E. Mucchi, A comparison among modal parameter extraction methods, *SN Applied Sciences* 1 (2019), p. 781. DOI: [10.1007/s42452-019-0806-8](https://doi.org/10.1007/s42452-019-0806-8)
- [12] R. J. Allemang, R. S. Patwardhan, M. M. Kolluri, A. W. Phillips, Frequency response function estimation techniques and the corresponding coherence functions: A review and update, *Mech. Syst. Signal Process.* 162 (2022), p. 108100. DOI: [10.1016/j.ymsp.2021.108100](https://doi.org/10.1016/j.ymsp.2021.108100)
- [13] Wolfram Research, LinearModelFit, Wolfram Language function, 2008. Online [Accessed 16 March 2024] <https://reference.wolfram.com/language/ref/LinearModelFit.html>